N.K. Balabaev, V.D. Lakhno,

A.M. Molchanov and B.P. Atanasov

7. EXTENDED ELECTRONIC STATES IN PROTEINS

A new approach to the problem of electron states in the protein molecule is developed. A "dielectric cavity" model of protein globule is used to study its extended states that basically are formed by the polarization field of the protein macromolecule. The size of such extended states in protein solutions can be compared with the size of protein globule. Possible role of these states in the charge transfer processes in biomacromolecules is discussed. The electron energies for the ground and the first excited states are calculated. The characteristic values of predicted energies of absorption and luminescence bands are found, ~1000 nm for the absorption band in the ground state and ~2000 nm for the luminescence band in the excited state. Various ways of experimental observation of such states are discussed.

1 Introduction

One of the central problems in molecular biology is the problem of long-distance electron transfer. At present, the fact of long-distance electron transfer in biological systems is well established. Theoretical studies in this field were stimulated by the work [1], where the temperature dependence of electron transfer rate from cytochrome c to chlorophyll was measured. The currently predominant point of view describes the mechanism of transfer as multitunnelling with unambiguous identifiable intermediates [2]. The theoretical foundations of electron transfer in application to biological systems were laid in the works of Foerster [3,4], Marcus [5], Jortner [6] and Hopfield [7,8], which in their turn were based on the idea of non-radiative electron transfer in condensed media, first developed by Peckar [9], Huang and Rhys [10]. The starting point of this idea was the suggestion about polaron states in condensed systems, which plays the central role in further development of electron transfer studies. It was a "polaronic" Hamiltonian that was used as a start

Excited Polaron States in Condensed Media.
Manchester: Manchester University Press, 1991.

in [9,10]. Thus, the achievements of the polaron theory in condensed systems can broaden our knowledge about electron states and transfer in biological systems.

The most general concept about polaron may be given in the following way. Let us consider an electron in a polar medium, where it shifts to an autolocalized state and does not form chemical bonds with the atoms of the medium. Such a state may be described as trapping of the electron by a potential well formed by electron-induced polarization of the surrounding molecules of the medium [9]. On this basis new results were obtained [11,12] according to which there is not only one but a whole set of discrete polaron states each having its corresponding potential well, self-consistent with the state of electron trapped in this well. An important principal consequence of these works is that even the first excited self-consistent polaron state has a large radius and can include (in the case of water, ammonia and other polar liquids) roughly 10^3- 10^4 and more molecules of the medium. These results also show that it is necessary to analyse the problem of long-distance electron transfer critically, namely to study its role in and impacts on biological systems. In this paper we consider states with large radii only in protein macromolecules. It will be shown that the assumption of the existence of electron states with large radii leads to many new results. The very fact of their existence suggests that new types of absorption and luminescence possibly occur in globule protein solutions. In the case of spherically symmetrical proteins with electron acceptor located in the globule centre the condition of formation of the excited polaron state with large radius implies isotropy of binary chemical reactions under photoexcitation.

In the present paper we would like to make consistent the representations of "polaron-in-condensed-medium" physics with the polaron properties of protein macromolecules. The simplest mathematical models of polaron states in proteins will be formulated and some of their consequences will be discussed.

2 Continuous Model

To introduce concepts about electron states with large radii in globular protein macromolecules it is necessary to examine continuous representations of these entities. It is also important to discuss the hierarchy of continuous models we will use. The representation of protein macromolecules (which takes spherical form in solutions) as micro phases included in solutions has been introduced in [13] on the basis of hydrophobic properties of protein. The development of electrostatic models of protein globules [14,15] led, in its turn, to their hierarchy. Fig.1 shows the simplest electrostatic model of protein globule, the dielectric cavity model. It assumes $\varepsilon_1 < \varepsilon_0$, which corresponds to low static dielectric permittivity of protein medium compared with highly polar solvent. One should stress that in the framework of this simplest model it is possible to explain qualitatively many

experimental results on protein transfer and electrophoresis [16]. Figure 2 presents a three-layer globule model. It takes into account the contributions of polar amino acid residues to dielectric permittivity in the region $R_1<r<R_2$ the penetration of water molecules into the surface layer, the surface unevenness, etc. We assume that solvent molecules cannot penetrate into the region $r<R_1$. In this model $\varepsilon_1<\varepsilon_2<\varepsilon_0$. The values of dielectric permittivity can be experimental ones, ε_1~4 corresponds to dielectric permittivity of NN-dimethilacetamid, a monomeric analog of peptide frame of protein (the tight region $r<R_1$, where the solvent molecules cannot penetrate); ε_0=80 corresponds to dielectric permittivity of water as a solvent.

The layer (R_1, R_2) is ascribed a mean value ε ~40 which in general is a model parameter. There is a great number of models which assume that dielectric permittivity inside the globule depends on coordinate ($\varepsilon=|\vec{r}|$ [17] et al.) and various nonlocal

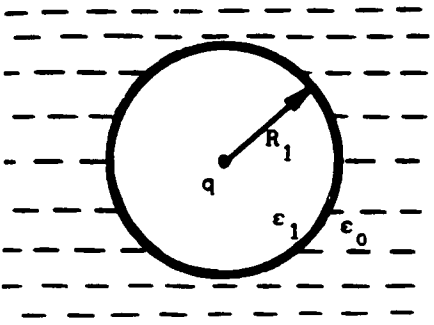

Fig.1. The two-layer model of the protein globule.

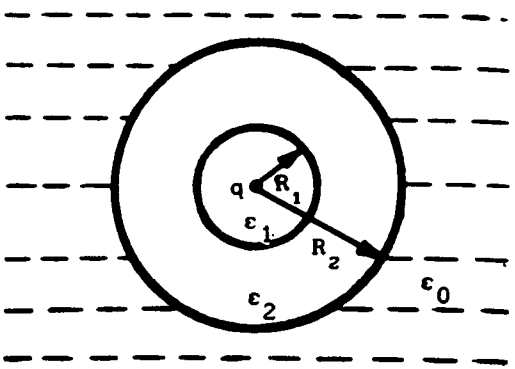

Fig.2. The three-layer model of the protein globule.

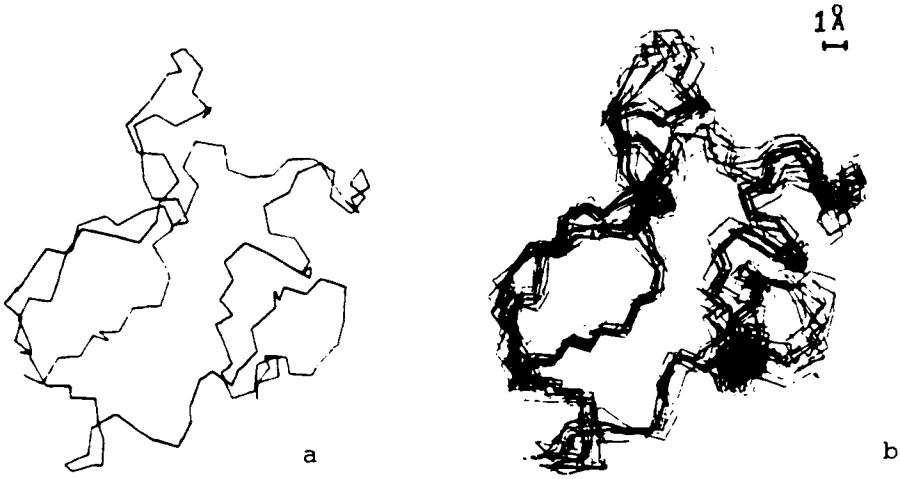

Fig.3. A plane projection of an instantaneous configuration of the ferredoxin molecule main chain $(-N-C^{\alpha}-C-)_{54}$ *(a); overlapped projections for 10 successive configurations of the molecule taken at a time interval* $\Delta t=0.6$ *picosec.*

models of dielectric cavity.

To establish a mathematical model of polaron-type electron states in the protein globule the most important parameter justifying the continuous approach is the ratio, $\langle r\rangle/\bar{a}$ where $\bar{a}$ is a mean distance between neighbouring atoms of the protein molecule, $\langle r\rangle$ is the effective radius of polaron. The estimation of $\bar{a}$ draws a clear distinction between a protein macromolecule and an ionic crystal, for the latter the condition $\langle r\rangle/\bar{a} \gg 1$ being the criterion of model continuity. In ionic crystals polarization is caused by small deviations of atoms from their equilibrium states, so that $\bar{a} \approx a$ (a is a lattice constant) whereas a protein macromolecule requires an additional averaging if the life time of the state in question is much longer than the characteristic time of oscillation of torsional degrees of freedom and deviations of macromolecule polar groups (usually less than 10^{-12} sec). This case is illustrated by Fig.3 based on the results of molecular dynamic computing experiment. Thus, for the long-lived states considered below the continuity condition is met in the case of protein globule much better than in the case of ionic crystals.

3 Polaron Model for Infinite Isotropic Medium (according to Peckar [9])

Polaronic description of an electron state in polar medium usually starts with the assumption that the mean Coulomb field induced by the excess electron locally polarizes the medium. The polarization electric field, in its turn, acts upon the electron [9]. It is essential that the electron interacts only with the inertial part of polarization it induces,

$$\vec{P}(\vec{r}) = \vec{P}_0(\vec{r}) - \vec{P}_\infty(\vec{r}) \tag{1}$$

where

$$\vec{P}_0 = \frac{\varepsilon_0 - 1}{4\pi\varepsilon_0}\vec{D}\ , \qquad \vec{P}_\infty = \frac{\varepsilon_\infty - 1}{4\pi\varepsilon_\infty}\vec{D}$$

are specific dipole moments of static and high frequency polarizations, ε_0 and ε_∞ are static and high frequency permittivities, respectively; $\vec{D}$ is the induction caused by the electron.

Thus,

$$\vec{P}(r) = \frac{\vec{D}(r)}{4\pi\tilde{\varepsilon}}\ , \tag{2}$$

$\tilde{\varepsilon}^{-1}=\varepsilon_\infty^{-1}-\varepsilon_0^{-1}$ is effective dielectric permittivity. The vector of electric induction caused by the distributed charge of electron with the density $e|\Psi(\vec{r})|^2$ is equal to

$$\vec{D}(\vec{r}) = e\int |\Psi(\vec{r}')|^2 \frac{\vec{r}-\vec{r}'}{|\vec{r}-\vec{r}'|^3}\, d\vec{r}'\ , \tag{3}$$

where $\Psi(\vec{r})$ is the wave function which can be determined from the solution of Sschrödinger equation

$$\frac{\hbar^2}{2\mu}\Delta\Psi(\vec{r}) + e\Pi(\vec{r})\Psi(\vec{r}) + W\Psi(\vec{r}) = 0\ , \tag{4}$$

where W is the energy of electron. The potential $\Pi(\vec{r})$ created by the electron-induced polarization $\nabla\Pi(\vec{r}) = 4\pi\vec{P}(\vec{r})$ is defined, according to (2) and (3) by the Poisson equation

$$\Delta\Pi(\vec{r}) + 4\pi\tilde{\varepsilon}^{-1}e|\Psi(\vec{r})|^2 = 0 \tag{5}$$

The system of nonlinear differential equations (4) and (5) totally determines the electron state in the infinite polar medium. To find the ground state of (4),(5), the variational principle has been used in [9]. In [11] the equations (4) and (5) have been integrated numerically and the solutions have been found corresponding to the excited polaron states different from the ground state. The approach developed in this section is used further to describe polaron states in the protein globule.

4 Equation for Polaron in the Protein Globule

The mathematical model of polaron states in the protein globule described by the dielectric cavity model is based on the following assumptions:

1) the globule is neutral, its effective surface charge on the layer boundaries being zero;
2) the electron states in the protein globule are considered as the states of polaron bound by the acceptor potential;
3) for each layer of the globule an isotropic model is assumed as well as corresponding smoothness conditions for the electron wave function and for the potentials inside each layer and on its boundary;
4) all the other assumptions are the same as those adopted for the description of polaron states in polar media [9].

In the case of spherical symmetry the assumptions 1)-4) yield the following equations for polaron in the protein globule

$$\frac{\hbar^2}{2\mu}\left(\frac{1}{r^2}\frac{d}{dr}\,r^2\,\frac{d}{dr}\right)\Psi(r)+e(\Pi(r)+\Phi(r))\Psi(r)+W\Psi(r) = 0 \tag{6}$$

$$\frac{1}{r^2}\frac{d}{dr}\,r^2\,\frac{d}{dr}\,\Pi(r) + \frac{4\pi e}{\tilde{\varepsilon}_i}\,\Psi^2(r) = 0 \tag{7}$$

$$R_{i-1} < r < R_i, \quad i=1,2\ldots; \quad R_0 \equiv 0, \tag{8}$$

where $\Phi(r)$ is the potential of acceptor

$$\Phi(r)=\begin{cases} q/\varepsilon_1 r+c_1, & r<R_1 \\ q/\varepsilon_2 r\ , & r>R_1 \end{cases} \tag{9}$$

for the two-layer model of the globule ($\varepsilon_2=\varepsilon_0$) and

$$\Phi(r)=\begin{cases} q/\varepsilon_1 r+c'_1, & r<R_1 \\ q/\varepsilon_2 r+c'_2, & R_1<r<R_2 \\ q/\varepsilon_3 r\ , & r>R_2 \end{cases} \tag{10}$$

for the three-layer model of the globule ($\varepsilon_3=\varepsilon_0$). $\Pi(r)$ is the potential of electron-induced polarization, μ is the effective mass of electron, $\tilde{\varepsilon}_i^{-1}=\varepsilon_\infty^{-1}-\varepsilon_i^{-1}$ are effective dielectric constants of the first layer, ε_∞ is the high frequency dielectric constant assumed identical for all the layers.

The natural boundary conditions for the equations (6),(7) follow from the conditions of boundedness and continuity of the wave function and the condition of potential continuity on the boundaries of the globule layers

$$\Psi'(0)+\frac{\mu qe}{\varepsilon_1\hbar^2}\Psi(0)=\Pi'(0)=0,\qquad \Psi(\infty)=\Pi(\infty)=0$$

$$\Psi(R_i-0)=\Psi(R_i+0),\qquad \Psi'(R_i-0)=\Psi'(R_i+0) \tag{11}$$

$$\Pi(R_i-0)=\Pi(R_i+0),\ \tilde{\varepsilon}_i\Pi'(R_i-0)=\tilde{\varepsilon}_{i\pm1}\Pi'(R_i+0)$$

The equation (6) is the Sschrödinger equation for the electron in the potential $-(\Pi+\Phi)$ which is defined in a self-consistent way by the equation (7). Thus, the nonlinear system of differential equations (6)-(7) with the boundary conditions (11) describes coupled polaron states in the protein globule. Its solution determines the wave function of electron state ψ, the energy of electron W and the total energy of state I_Φ given by the functional

$$I_F[\Psi,\Pi]=\frac{\hbar^2}{2\mu}\int(\nabla\Psi)^2d\vec{r}-e\int\Psi^2(\Pi+\Phi)d\vec{r}+\sum_i\frac{\tilde{\varepsilon}_i}{8\pi}\int_{\Omega_i}(\nabla\Pi)^2d\vec{r} \tag{12}$$

In the last term of (12) the integration is carried out over the Ω_i regions that correspond to the layers of dielectric cavity model. Note that the equations (6),(7) can be obtained by an independent variation of the functional (12) over the wave function $\psi(r)$ and the potential $\Pi(r)$ taking into account the normalization of the wave function $\int\Psi^2(\vec{r})d\vec{r}=1$.

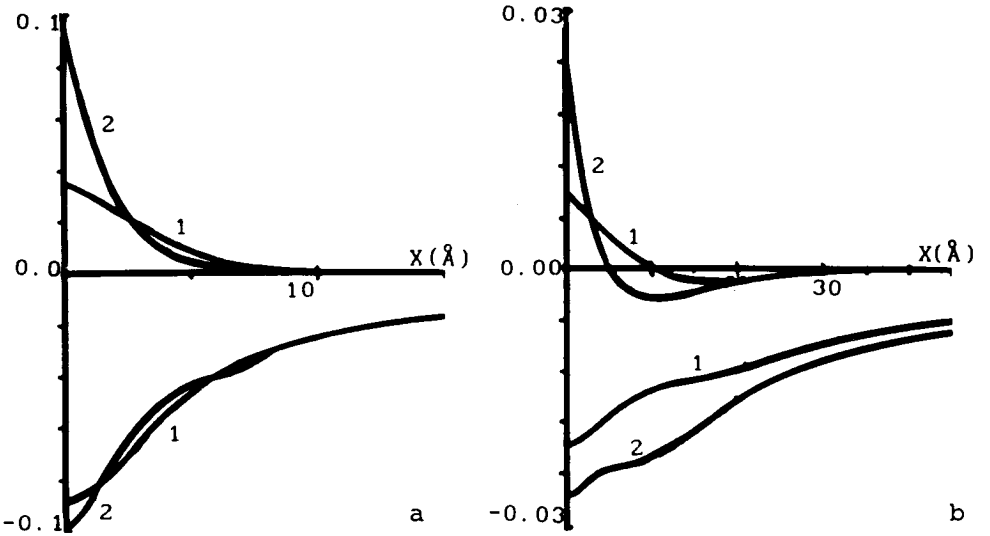

Fig 4. Solution of the (6)-(7) problem for the two-layer (1) and three-layer (2) model of the protein globule, a is zero mode, b is first mode; the functions $\psi(X)$ $\int 4\pi X^2\psi^2 dX=1$ *and* $\Pi(X)\frac{\hbar^2}{\mu e^3}$ $(\approx 0.09\Pi(X))$ *are shown in the upper and the lower part of Fig.4, respectively.*

5 Solutions of the Polaron Equations. Ground State

The system of equations (6) - (7) can be integrated numerically. The algorithm of finding the solution of (6) - (7) is described in detail in the Appendix. In the case of uniform polar media (all $\varepsilon_i=\varepsilon_0$) a problem of F-centre in the ionic crystal is obtained. It was solved in [12]. As is shown in the Appendix, the system of equations (6) - (7) has a discrete set of solutions, which comprise the self-consistent electron states and polarization of globule and its surrounding. The solution without nodes, which corresponds to the ground state (zero mode) is shown in Fig.4a, the solution with a node which corresponds to excited self-consistent state (1st mode) is shown in Fig.4b. In this section we will discuss only the results corresponding to the ground state.

Table 1 gives the following values corresponding to the ground self-consistent state (for the two- and three-layer model), electron energy W_{1S} and total energy I_{1S} non-selfconsistent electron levels in 2S (W_{2S}) and 2P (W_{2P}) states and total energies that correspond to them (I_{2S}, I_{2P}) as well as the state radii ($\langle r\rangle_{1S}$, $\langle r\rangle_{2P}$, $\langle r\rangle_{2S}$).

The table shows that for the more realistic three-layer model the radius of polaron in the ground state $\langle r\rangle_{1S}=2,3\overset{o}{A}$ i.e. beyond the continuum model approximation. Accordingly, the value $\Delta W_{1S,2P}=|W_{2P}-W_{1S}|\simeq 1,2eV$ gives an approximate evaluation of transfer energy to which the absorption band of maximum would correspond. These bands' position according to the evaluation 1,2eV (~1000 nm) is just in the region of charge transfers of metal-containing proteins [19].

6 Excited Polaron State in the Protein Globule

Table 1 also lists (for the two- and three-layer model of dielectric cavity) the values of electron energies (W), total energies (I) and radii <r> in the excited selfconsistent state (2S) and in non-selfconsistent states 1S and 2P that correspond to the potential polaronic well 2S (Fig 4b).

Table 1. Characteristics of polaron states in the protein globule.

Physical[1] value	Two-layer model[2]		Three-layer model[3]	
	0-mode	1-mode	0-mode	1-mode
W_{1S}	-1,316	-0,401	-2,200	-1,035
W_{2S}	-0,529	-0,256	-0,697	-0,424
W_{2P}	-0,695	-0,283	-0,806	-0,413
I_{1S}	-0,508	-0,238	-1,243	-0,779
I_{2S}	0,280	-0,093	0,255	-0,169
I_{2P}	0,114	-0,120	0,146	-0,158
$\langle r\rangle_{1S}$	3,7	8,3	2,3	3,1
$\langle r\rangle_{2S}$	10,0	19,5	7,6	12,2
$\langle r\rangle_{2P}$	6,8	16,0	5,7	11,0

1) The values of energies W_{1S}, W_{2S}, W_{2P} and I_{1S}, I_{2S}, I_{2P} are in eV; the avareged radii $\langle r\rangle_{1S}, \langle r\rangle_{2S}, \langle r\rangle_{2P}$ -in $\overset{\circ}{A}$.

2) $\varepsilon_1 = 20$, $\varepsilon_2 = 80$, $\varepsilon_\infty = 2$, $R_1 = 15\overset{\circ}{A}$, $\mu = m_o$, $Z = 1$.

3) $\varepsilon_1=4$, $\varepsilon_2=40$, $\varepsilon_3=80$, $\varepsilon_\infty=2$, $R_1=7\overset{\circ}{A}$, $R_2=15\overset{\circ}{A}$, $\mu=m_0$, $Z=1$.

First of all note that for both two- and three layer models, the radii of excited selfconsistent state (19,5 Å and 12,2 Å, respectively) greatly exceed the mean distance between neighbouring atoms a of the medium, i.e. the continuous approximation is quite accurate in this case. Our calculations show that the energies of electron in selfconsistent 2S and in non-selfconsistent 2P states are close to each other. In the case of a three-layer model, the 2P state has a higher energy level than the 2S state. Since the dipole transition to the 2S state is allowed only from the 2P state, we can expect for the three-layer model a longer lifetime of the excited selfconsistent 2S state.

The table also gives an approximate estimate for the luminescence band for the three-layer model: $\Delta W_{2P,1S}$=0,61eV (~2000 nm), i.e. it lies in the far infrared region. It would be interesting to watch such a band experimentally, its identification as a polaron could be carried out on the basis of preliminary evaluation of qualitative impact of pH, the ionic strength and temperature on the qualities of the "polaron" bands.

7 Dielectric Cavity Model and the Theory of Electron Transfer

It follows from what is stated above that the electrostatic model of the protein globule can also be used for the description of various processes of photoexcitation and electron transfer. Thus, the probability ω of electron in the excited 2S selfconsistent state of the protein molecule tunneling from donor to acceptor is given by the expression [6,8,20,21]:

$$\omega = L^2 \exp\left(-\frac{E_r}{\bar{\omega}}\right)(\pi/E_r T)^{1/2} \exp(-(E_r - J)^2/4E_r T) \qquad (13)$$

$$E_r = 1/8\pi\tilde{\varepsilon} \int |\vec{D}_{2S} - \vec{D}_{acs}|^2 \, d\vec{r} \,,$$

where L is the matrix element of tunnelling; $\vec{D}$ is determined from (3); J is the reaction heat, $\bar{\omega}$ is the mean frequency of polarization oscillations of the molecule, E_r is the energy of medium reorganization. The values L and D_{acs} can be calculated only if the acceptor model is defined.

From (13) it follows in particular that in the electrostatic model considered here the tunnelling probability that is proportional to the reaction rate depends upon the kind of electron states via the tunnelling matrix element L and inductions $\vec{D}_{2S}$ and $\vec{D}_{acs}$. In the case of extended electron states one can expect the dependence of the reaction rate constant on the pH of solution and on spatial distribution of charged amino acid groups

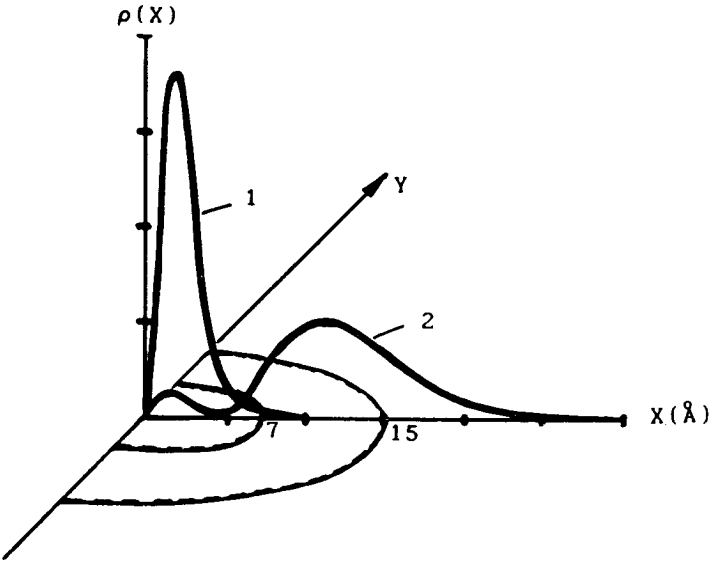

Fig.5. Distribution of electronic density in the protein globule (the three-layer model described in Section 2); $\rho(X)=4\pi x^2\psi^2(X)$; 1 is zero mode, 2 is first mode.

via the induction $\vec{D}_{2S}|\psi|$ (equation (3)) dependable on the polaron wave function which embraces the most polarizable parts of the protein molecule in the layer (R_1,R_2) of our model (Fig.5).

8 Discussion

The idea of extended states with large radii introduced in this paper paves the way for a quite new approach to the problem of long-distance electron transfer. According to the results of the 4th and 5th sections for the dielectric cavity model, the radius of the first excited selfconsistent state can be compared with the globule size. It means that the whole globule is involved in the formation of such a state. If the acceptor is near the globule and the extended selfconsistent state has roughly the same energy as the electron state of the acceptor then it is hardly possible to tell whether the electron belongs to the globule or to the acceptor. In the case when the distance between the acceptor and the globule is large, the value of the tunnelling matrix element L (see (13)) is of paramount importance. For the states of large radii its value may be several orders higher than that of a small-radius state.

Each excited selfconsistent state can be related to configurational coordinates. For a consistent description of electron transfer one should take into account that during the

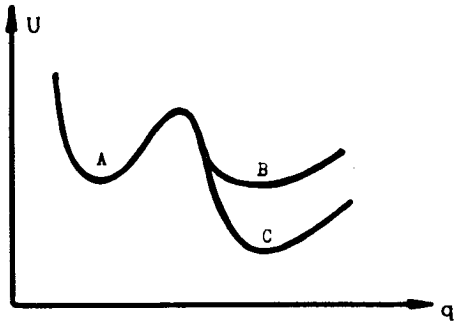

Fig.6. A simplest branching scheme of the electron transfer configuration coordinate q.

transfer process the electron can jump to intermediate selfconsistent states of the acceptor and then to the ground state. Thus, a complex picture of electron transfer with branching of the reaction coordinate becomes feasible (Fig.6).

The simplest case shown in the figure, i.e. the transition from the state B to C can be either radiative or non-radiative; in the more general cases, the cascade radiative and non-radiative processes are possible.

The existence of excited selfconsistent states may lead to interesting peculiarities in the lines of EPR, NMR, IR absorption spectra and others. They can be used for identification of such states. The discussion of these questions, however, is beyond the scope of this paper.

Appendix

Finding the Polaron States in the Globule

1^{o}. We shall seek spherically symmetrical solutions of differential equations (6)-(7) with boundary conditions (11) for the globule models shown in Figs.1 and 2. For that purpose we introduce new variables

$$r = \frac{\hbar}{(2\mu|W|)^{1/2}} X , \quad \Psi(r) = \frac{|W|}{e\hbar} \left(\frac{\mu\tilde{\varepsilon}_o}{2\pi} \right)^{1/2} Y(X) ,$$

$$\Pi(r) = \frac{|W|}{e} Z(X) \qquad (A1)$$

From the condition of wave function normalization one obtains

$$|W| = \frac{2\mu e^4}{\hbar^2 \tilde{\varepsilon}_0^2} \frac{1}{\Gamma^2}, \qquad \text{where} \qquad \Gamma = \int_0^\infty Y^2(X) X^2 dX$$

(A1) can then be rewritten as

$$r = \frac{\hbar^2}{2\mu e^2} \tilde{\varepsilon}_0 \Gamma X, \qquad \Psi(r) = \left(\frac{2}{\pi}\right)^{1/2} \mu^{3/2} e^3 \hbar^{-3} \frac{Y(X)}{\Gamma^2 \tilde{\varepsilon}_0^{3/2}},$$

$$\Pi(r) = \frac{2\mu e^3}{\hbar^2} \frac{Z(X)}{\Gamma^2 \tilde{\varepsilon}_0^2} \qquad \text{(A1')}$$

Also we introduce the notation $\Phi(r) = \frac{|W|}{e} \hat{\Phi}(X)$.

Substituting (A1) into (6) and (7) we obtain equations with spherically symmetrical solutions

$$\frac{d^2Y(X)}{dX^2} + \frac{2}{X} \frac{dY(X)}{dX} + Y(X)(Z(X) + \hat{\Phi}(X) - 1) = 0$$

$$\frac{d^2Z(X)}{dX^2} + \frac{2}{X} \frac{dZ(X)}{dX} + æ(X) Y^2(X) = 0 \qquad \text{(A2)}$$

For the two-layer model of the globule (Fig.1):

$$\hat{\Phi}(X) = \begin{cases} \frac{N}{X} \frac{\varepsilon_0}{\varepsilon_1} + \frac{N}{X_R} \left(1 - \frac{\varepsilon_0}{\varepsilon_1}\right), & X < X_R \\ \frac{N}{X_R}, & X \geq X_R \end{cases}$$

where X_R is the dimensionless radius of the globule

$$R = \frac{\hbar^2}{2\mu e^2} \tilde{\varepsilon}_0 \Gamma X_R$$

The new parameter N is proportional to the charge q=Ze:

$$N = \left(\frac{2\mu}{|W|}\right)^{1/2} \frac{eq}{\hbar\varepsilon_0} = \Gamma Z \frac{\tilde{\varepsilon}_0}{\varepsilon_0}$$

The piecewise-constant function æ(X) breaks on the surface of the globule

$$æ(X) = \begin{cases} \tilde{\varepsilon}_0/\tilde{\varepsilon}_1 , & X < X_R \\ 1 , & X \geq X_R \end{cases}$$

Analogously, for the three-layer model (Fig.2)

$$\hat{\phi}(X) = \begin{cases} \frac{N}{X}\frac{\varepsilon_0}{\varepsilon_1} + \frac{N}{X_{R_1}}\left(\frac{\varepsilon_0}{\varepsilon_2} - \frac{\varepsilon_0}{\varepsilon_1}\right) + \frac{N}{X_{R_2}}\left(1 - \frac{\varepsilon_0}{\varepsilon_2}\right) , & X < X_{R_1} \\ \frac{N}{X}\frac{\varepsilon_0}{\varepsilon_2} + \frac{N}{X_{R_2}}\left(1 - \frac{\varepsilon_0}{\varepsilon_2}\right) , & X_{R_1} \leq X \leq X_{R_2} \\ \frac{N}{X} , & X > X_{R_2} \end{cases}$$

$$æ(X) = \begin{cases} \tilde{\varepsilon}/\tilde{\varepsilon}_1 , & X < X_{R_1} \\ \tilde{\varepsilon}/\tilde{\varepsilon}_2 , & X_{R_1} \leq X < X_{R_2} \\ 1 , & X \geq X_{R_2} \end{cases}$$

The solutions of equations (A2) must satisfy the conditions on infinity that follow from (11), be bounded at zero and meet the corresponding internal boundary conditions at break points of the piecewise-constant function æ(X).

The boundary conditions for the equations (A2) have the form

$$2Y'(0) + N\frac{\varepsilon_0}{\varepsilon_1} Y(0) = Y(\infty) = 0, \qquad Z'(0) = Z(\infty) = 0 \qquad (A3)$$

For the internal boundary conditions the following relations can be written

$$Y(X_{R_i}-0)=Y(X_{R_i}+0), \quad Y'(X_{R_i}-0)=Y'(X_{R_i}+0)$$

$$Z(X_{R_i}-0)=Z(X_{R_i}+0), \quad \tilde{\varepsilon}_i Z'(X_{R_i}-0)=\tilde{\varepsilon}_{i+1} Z'(X_{R_i}+0) \tag{A3'}$$

Here i=1 for the two-layer model of the globule ($R_1=R$, $\tilde{\varepsilon}_2=\tilde{\varepsilon}_0$) and i=1 and 2 for the three-layer model ($\tilde{\varepsilon}_3 \equiv \tilde{\varepsilon}_0$).

2^o. The solutions of the problem (A2) with the boundary conditions (A3) and internal boundary conditions (A3') were found in the same way as in the problem of polaron in a homogeneous polar medium /11/ and in the F-centre problem /12/. Moreover, to find the polaron states in the globule the solutions for the F-centre problem were used.

The procedure of solution finding is obvious for the problem of polaron in a homogeneous polar medium, so here we will describe the algorithm for just this case. Further we show how the problems of our interest could be dealt with.

2.1. The equations for a polaron in the homogeneous media can be regarded as a particular case of the (A2) equations, when $\varepsilon_1=\varepsilon_0$ and N=0. The mathematical formulation is reduced to finding the solutions of the boundary problem

$$Y''(X) + \frac{2}{X} Y'(X) + Z(X)Y(X) - Y(X) = 0$$

$$Z''(X) + \frac{2}{X} Z'(X) + Y^2(X) = 0 \tag{A4}$$

$$Y'(0)=Z'(0)=0; \quad Y(\infty)=Z(\infty)=0$$

It has been shown in /11/ that this problem has a set of solutions of the following character: $z_n(X)$ (n=0,1,2... where n is the solution number) tends to zero monotonically as $X\to\infty$, and $Y_n(X)$ crosses the X axis n times, then approaches zero as $X\to\infty$.

Now we change variables ($\xi=XY$, $\eta=XZ$) and the equation (A4) takes the form

$$\xi''+ \xi(\eta/X - 1) = 0$$

$$\eta''+ \xi^2/X = 0 \tag{A5}$$

$$\xi(0)=\eta(0)=0; \quad \xi(\infty)=\eta'(\infty)=0 \tag{A6}$$

2.2. The solutions of the (A5) system satisfying only the left-hand boundary condition (A6) may be presented in the neighbourhood of the point X=0 as power series

$$\xi(X) = a_1X + a_2X^2 + a_3X^3 + \ldots$$

$$\eta(X) = b_1X + b_2X^2 + b_3X^3 + \ldots$$

Substituting these series into (A5) one finds that all coefficients a_i and b_i can be expressed in terms of $a_1 \equiv a$ and $b_1 \equiv b$. Confining ourselves to theseveral first terms of the series, we can, at a point X_0 which is not distant from the point X=0, find with desired accuracy the values of $\xi(X_0,a,b)$ and $\eta(X_0,a,b)$ and their derivatives corresponding to concrete values of a and b parameters.

2.3. For the system of differential equations (A5) we define the Cauchy problem in the interval $[X_0,X_K]$. For this purpose, $\xi(X_0,a,b)$, $\xi'(X_0,a,b)$, $\eta(X_0,a,b)$ and $\eta'(X_0,a,b)$ are calculated at $X=X_0$ (X_0 is small) with the given values of parameters a and b. Then the solution of the Cauchy problem is found numerically on a computer using the standard Runge-Kutta method.

Note that the second equation of the system (A5) yields a convex function $\eta(X)$, $\eta''(X)<0$ for all $X\geq 0$. This property of $\eta(X)$ is crucial for constructing an algorithm of boundary problem solution. If the values of a and b parameters are chosen so that the solution of $\eta(X)$ tends to a constant at $X\to\infty$ then $\xi(X)$ will also tend to zero. Thus, one of the solutions for the boundary problem (A5)-(A6) is found.

2.4. Now we take an interval $[X_0,X_K]$ and, giving different values to a and b parameters, begin to solve the Cauchy problems corresponding to them. Figure 4 shows some of the solutions. Choose an X_K corresponding to the maximum of such a solution for which $a=a^*$ and $b=b^*$ (a^* and b^* are concrete numbers). Define the function

$$F(a,b)\equiv\eta'(X_K,a,b).$$

Now we shall solve the Cauchy problem on a new interval $[X_0,X_K]$. Taking different values of a and b parameters and solving the corresponding Cauchy problem we thus calculate the values of the

function F(a,b). The equation

$$F(a,b)=0 \tag{A7}$$

implicitly defines a dependence between a and b parameters. Here, because of the choice of X_K, one point of this dependence is known in advance, namely,

$$F(a^*,b^*)=0.$$

The dependence (A7) in the given intervals of a and b parameters can be found using the CURVE program /22/. Figure 8 shows a dependence thus obtained.

The solutions of the Cauchy problem for the different values of a and b parameters taken consecutively along the curve are shown in Fig.9. Analysis of the curves $\xi(X)$ suggests the existence of a set of boundary problem (A5)-(A6) solutions. They may be arranged in the following way: $\xi_n(X)$ (n=0,1,2...) crosses the X axis n times and then approaches zero exponentially; $\eta_n(X)$ rises monotonically to its extreme value $\eta_n(\infty)$.

2.5. Now we define a system of two functions of three variables

$$F_1(a,b,X_K) \equiv \xi'(X_K;a,b)$$
$$F_2(a,b,X_K) \equiv \eta'(X_K;a,b) \tag{A8}$$

This definition means that, in order to find the values of functions F_1 and F_2, the Cauchy problem is solved in the interval $[X_0,X_K]$ with the initial conditions corresponding to the values of a and b parameters. The values of ξ' and η' at the end of the integration interval determine the values of the function. The system of equations

$$F_1(a,b,X_K) = 0$$
$$F_2(a,b,X_K) = 0 \tag{A9}$$

determines a curve in the space of variables a, b and X_K. We have found pieces of several curve branches. To do this, we chose initial approximations to the corresponding curve branch and the

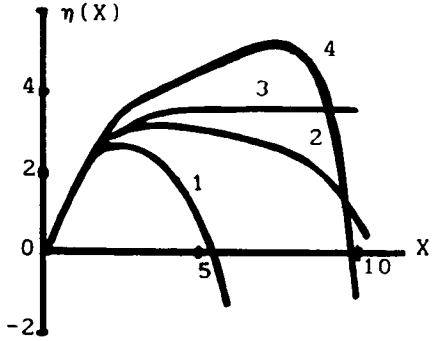

Fig.7. Functions η(X) for the different initial data determined by a and b parameters, 1: a=1.2, b=2.0; 2: a=1.1, b=2.0; 3: a=1.02, b=1.94; 4: a=1.0, b=2.0.

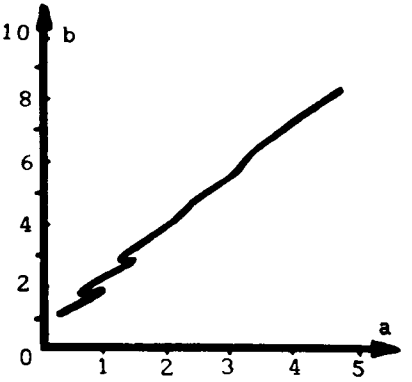

Fig.8. The dependence between the parameters a and b following from (A6) at X_K=10.

CURVE program found the points on the corresponding branch of the (A9) curve in the given interval of the parameters a, b and X_K.

At $X_K \to \infty$, the conditions (A9) are identical to the right-hand boundary conditions (A6). In fact, in the polaron problem, it was enough to go up to X_K=10 for the zero mode (n=0), X_K=15 for the first mode (n=1) and X_K=20 for the second mode (n=2) to obtain the boundary problem solutions accurate to several figures.

Fig. 10 shows two solutions of those boundary problems obtained by the procedure just described.

3°. The problem of F-centre differs from the problem of polaron in a homogeneous polar media in additional terms of the sum NY/X in the first of the equations (A3), where N is the problem parameter. The solutions for different values of N were sought on the corresponding curves that pass through the polaron solutions.

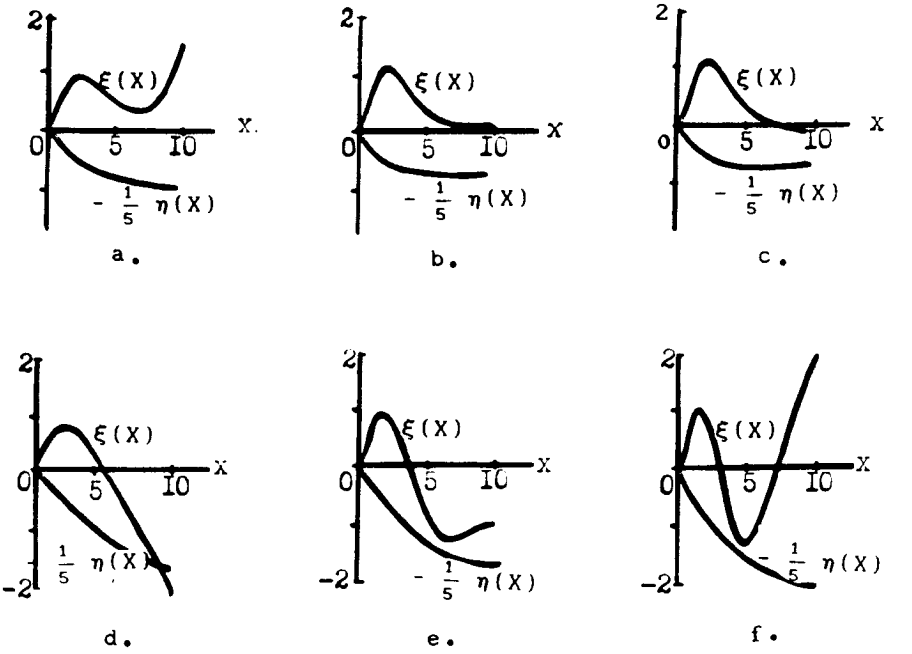

Fig.9. The solutions of the Cauchy problem for the different values of a and b on the curve (A9). a=0.733, b=1.664 (a); a=1.003, b=1.921 (b); a=1.025, b=1.942 (c); a=0.623, b=1.662 (d); a=0.900, b=2.074 (e); a=1.338, b=2.727 (f).

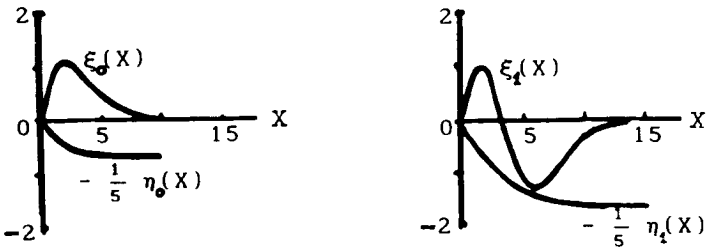

Fig.10. The solutions of the boundary problem (A5)-(A6): a=1.021, b=1.938 (a); a=1.091, b=2.320 (b).

Let us write down the system of equations

$$F_1(N,a,b) \equiv \xi'(X_K;N,a,b) = 0$$

$$F_2(N,a,b) \equiv \eta'(X_K;N,a,b) = 0 \qquad \text{(A10)}$$

The known values at N=0 for polaron states were chosen as initial points lying on the curve (A10). The dependences themselves were calculated by the CURVE program . To refine the solution at the given N, new functions were introduced

$$F_1(a,b,X_K) \equiv \xi'(X_K;N,a,b)$$

$$F_2(a,b,X_K) \equiv \eta'(X_K;N,a,b)$$

Then the procedure analogous to that used in the case of polaron for the system (A9) was repeated.

4°. The problems of polaron and F-centre in a homogeneous polar media considered above give an idea how to find spherically symmetrical polaron states in different models of the protein globule. Let us analyse the case of the two-layer model (Fig.1). Finding the solutions for the case of multi-layer model differs only in "technical" details.

The initial model (Section 4) takes the values $\{\varepsilon_1,\varepsilon_2,\varepsilon_\infty,R,Z\}$ as physical parameters. In the boundary problem, (A2)-(A3) there are X_R and N instead of R and Z, with the relationships between them

$$X_R = R\,\frac{2\mu e^2}{\tilde{\varepsilon}_0 \hbar^2}\,\Gamma^{-1}$$

$$N = Z\,\frac{\tilde{\varepsilon}_0}{\varepsilon_0}\,\Gamma \qquad \text{(A11)}$$

Since the value $\upsilon = \int_0^\infty Y^2(X)X^2dX$ is not known in advance, the values of parameters X_R and N that correspond to the given globule radius R and the charge Z are also unknown. Their product though is known

$$NX_R = \frac{2\mu e^2}{\hbar^2}\,\frac{RZ}{\varepsilon_0} = \text{const} \qquad \text{(A12)}$$

In the right-hand part of (A12), there are only the universal constants and model parameters. The dependence (A12) suggests the following scheme of solution finding.

Step 1. We go over to the variables $\xi=YX$, $\eta=ZX$. Representing $\xi(X)$ and $\eta(X)$ as power series.

$$\xi(X) = a_1X + a_2X^2 + \ldots$$

$$\eta(X) = b_1 X + b_2 X^2 + \ldots$$

and substituting them into (A2) we find a two-parameter family of the (A2) solutions in the neighbourhood of the point X=0 that satisfy the left-hand boundary condition (A3). The parameters a_1 and b_1 are equal to $Y(0)=Y_0$ and $Z(0)=Z_0$, respectively.

Step 2. We start from the known equations of the F-centre problem. Let Y_0^*, Z_0^* and N_0^* be the values of system parameters that determine a mode of the F-centre. According to (A12), X_R^*= const/N^*. The system of equations is defined as follows

$$F_1(Y_0,Z_0,\varepsilon_1) \equiv \xi'(X_K;Y_0,Z_0,\varepsilon_1) = 0$$

$$F_2(Y_0,Z_0,\varepsilon_1) \equiv \eta'(X_K;Y_0,Z_0,\varepsilon_1) = 0 \qquad \text{(A13)}$$

Let ε_1=80 and N=N^*. Then the point $(Y_0,Z_0,\varepsilon_1)=(Y_0^*,Z_0^*,\varepsilon_0)$ lies on the curve (A13) because of the choice of initial parameter values. One may use the CURVE program to locate the curve branch passing through this point. Thus, it is possible to advance from ε_1=80 to ε_1=20 which was found in the two-layer model.

Step 3. Let us define the system of equations

$$G_1(Y_0,Z_0,N) \equiv \xi'(X_K;Y_0,Z_0,N) = 0$$

$$G_2(Y_0,Z_0,N) \equiv \eta'(X_K;Y_0,Z_0,N) = 0 \qquad \text{(A14)}$$

Starting from the previous solution with ε_0=80, ε_1=20 and the corresponding values of parameters Y_0, Z_0, N we locate the curve branch with the help of the CURVE program. For each point found lying on the curve we calculate $\Gamma = \int_0^\infty Y^2X^2dX$ and then

$$R = X_R \Gamma \frac{\hbar^2 \varepsilon_0}{2\mu e^2} \quad \text{and} \quad Z = \frac{N}{\Gamma} \frac{\tilde{\varepsilon}_0}{\varepsilon_0} .$$

This procedure along the curve is carried out until the model parameters R=15Å and Z=1 are reached (because of (A12) it will happen simultaneously). Thus, the solution of the boundary problem for the globule model in question will be found.

Step 4. If necessary, the solution can be refined, making X_K a parameter and moving along it to the greater values. The examples of solutions for the polaron states in the globule are shown in Fig.4.

Step 5. To find the spectral characteristics of electron in the potential field of selfconsistent polaron states, the linear Sschrödinger equation has been solved with the potential $U(X)=Z_n(X)+\Phi(X)$ where $Z_n(X)$ is the n-th solution of the boundary problem. However, some difficulties arise here because the function $z_n(X)$ is defined only on a discrete sequence of unevenly distributed points. In such cases it is a common practice to use interpolation formulae. We tried another way. Namely, to the linear Sschrödinger equation

$$\zeta'' - \frac{l(l+1)}{X^2} \zeta + \zeta\left(\frac{\eta}{X} + \hat{\Phi}\right) - \lambda\zeta = 0 \qquad \text{(A15)}$$

the following equations for polaron states were appended

$$\xi'' + \xi(\eta/X + \hat{\Phi}) - \xi = 0$$

$$\eta'' + æ(X)\xi^2/X = 0 \qquad \text{(A16)}$$

and these three equations were considered as a system of differential equations. The variable ζ is not included in (A16), so each time $\eta(X)$ from (A15) is reproduced unaltered (corresponding to the polaron mode and at the points conforming to (A15)). It does not depend upon the values and initial data for $\zeta(X)$. For the given l (orbital moment) and n (number of zeros), λ was found by the halving procedure. The results of calculations are presented in Table 1.

References

[1] De Vault, Chance B. Photosynthesis using a pulsed laser.1. Temperature dependance of cytochrome oxidation rate in chromatium - Evidence for tunnelling. - *Biophys.J.*, (1966), **v.6**, p.825-847.

[2] Tunnelling in biological systems (Ed. Chance B.) - N.Y.;

Acad.press, (1979), 386p.
[3] Forster T. - *Naturwissenchaften*, (1946), **v.33**, p.166.
[4] Forster T. - *Discuss. Faraday Soc.*, (1959), **v.27**, p.7.
[5] Marcus R.A. Chemical and electrochemical electron transfer theory. - *Ann.Rev.Phys.Chem.*, (1964), **v.15**, p.155.
[6] Jortner J. Temperature dependent activation energy for electron transfer between biological molecules. - *J.Chem.Phys.*, (1976), **v.64**, No12, p.4860-4867.
[7] Hopfield J.J. Electron transfer between biological molecules by thermally activated tunnelling. - *Proc.Nat.Acad.Sci.* USA, (1974), **v.71**, No9, p.3640-3644.
[8] Hopfield J.J. Photo-induced charge transfer. A critical test of the mechanism and range of biological electron transfer processes. - *Biophys.J.*, (1977), **v.18**, p.311-321.
[9] Peckar S.I. Studies into the electron theory of crystals. Moscow: Gostechizdat, (1951).
[10] Huang, K., Rhys, A. *Proc. Roy. Soc.* (1950) **v.204**, p.406; The theory of optical and nonradiatory transitions in the F-centre. Problems of Semiconductor Physics. Moscow: IL, 1957.
[11] Balabaev, N.K., Lakhno, V.D. Soliton solutions in the polaron theory. *Theor. and Math. Phys. (USSR)*, (1980), **v.45**, No. 1, p. 139.
[12] Lakhno, V.D., Balabaev, N.K.. Self-consistent states in a continual model of the F-centre and the problem of the relaxed excited state. *Optics and Spectrosxopy (USSR)* (1983), **v.43**, No. 7, p. 326-330.
[13] Bresler, S.E., Talmud, D.L. On the nature of globular proteins. *Proc. Acad. Sci. USSR*, (1944), **v.43**, No. 7, p. 326-330.
[14] Tenford C., Kirkwood J.G. Theory of protein titration curves 1,11. General equations for unpenetrable spheres. - *J.Am.Chem.Soc.*, (1957), **v.79**, p.5333-5339.
[15] Mattew J.B. Electrostatic effects in proteins. - *Ann.Rev.Biophys. Chem.*, (1985), **v.14**, p.387-417.
[16] Tanford C. Physical Chemistry of polymers. Moscow: Chimia, 1965.
[17] Rogers K. The modelling of electrostatic interactions in the function of globular proteins. - *Progress in biophysics and molecular biology*, (1986), **v.48**, No1, p.37-66.
[18] Kornyshev A.A., Dogonadze R., Ulsirup J. - In: The Chemical Physics of Solvation, PT.A., Amsterdam; Elsevier, 1985, p.70-116.
[19] Leninger, A.L. Biochemistry. The molecular basis for structure and function. N.Y.: Worth Publishers, 1972.
[20] Zamaraev, K.I., Khayrutdinov, P.F., Zhdanov, V.P. Tunnelling of electron in chemistry. Moscow: Nauka, 1975.
[21] Petrov, E.G. Physics of electron transfer in biosystems. Kiev: Naukova Dumka, 1984.
[22] Balabaev, N.K., Lunevskaya L.V. Motion along the curve in an n-dimensional space. FORTRAN algorithms and Programs. Preprint. Pushchino, 1978.